Experiment-Based Methodology of Kinetic Battery Modeling for Energy Storage

Article *in* IEEE Transactions on Industry Applications · August 2018

DOI: 10.1109/TIA.2018.2866148

4 authors, including:

Nouhou Bako Zeïnabou
Université Paris-Est Créteil Val de Marne - Université Paris 12

Seidou Maiga Amadou
Gaston Berger University, Saint-Louis

Experiment-based Methodology of Kinetic Battery Modeling for Energy Storage

Z. Nouhou Bako[1], M.Abdou Tankari[2], G. Lefebvre
CERTES Lab., University of Paris-Est Creteil,
61, Av. du Général De Gaulle, 94010, France
[1]zeinabou.bako@uddm.edu.ne, [2]mahamadou.abdou-tankari@u-pec.fr

A. Seidou Maiga
EITER Laboratory, Gaston Berger University,
BP 234 - Saint-Louis, Senegal
amadou-seidou.maiga@ugb.edu.sn

***Abstract*— this paper presents a methodology of the battery modeling based on experimental tests results. As main contribution, authors conducted an analysis of the main constraints and effects of each parameter of the batteries model on its behavior and lifetime. This can help to improve the accuracy of the model. Due to its capability to model the recovery effect and the rate-capacity one, the Kinetic Battery Model serves as basis of the study. Results of experimental tests are used to realize the analysis and to define the suitable methodology of batteries parameters identification. These last can serve for prediction and estimation of the battery lifetime according to the actual operating conditions, particularly in microgrid and distributed systems.**

Keywords—Kinetic Battery Model; Modelling; Lead-acid battery, Energy storage; Characterization; Experimental tests.

I. Introduction

Nowadays, there are several challenges concerning the energy production and consumption over the world [1][2]. The innovative and promising ways are related to the smart grid that are based on the mixing of the energy sources and storage devices [3]–[6][29]. So, the combination of different kind of renewable and fossil energy can help to reduce de gas emission and global warming. But, this objective is facing on several constraints such as the investment costs, the hard variations of energy resources, and the difficulties in prediction of the renewable productions that can affects the system autonomy. For these reason, the energy storage become an interesting alternative to improve the energy availability and to solve the problem of correlation between production and consumption.

Conditions of batteries tests conducted by the manufacturers are generally very different to the actual operations. So, the predicted lifetime can be very short than the previous one [7]–[10][32]. Knowledge of renewable energy system shows that a battery's lifetime is drastically reduced by the intermittencies of the operating power. An accurate model is required for online estimation of the batteries performances and lifetime, in aim to ensure the power supply availability and efficiency, particularly in autonomous system.

In this paper a methodology of battery modeling based on the "Kinetic Battery Model (KiBaM)" is presented and illustrated through experimental tests, performed by authors. The behavior of the batteries and their performances are studied and the simulation model is established. From the resulting knowledge, the batteries failures and damage mechanisms can be estimated for lifetime improving according to the actual operating conditions of the batteries. The main advantages of the Kinetic Battery Model is due to their ability to model the recovery effect of the battery and the rate-capacity one [27]. This paper presents an analysis that can help to establish an accurate model of lead-acid and lithium-ion batteries.

II. Kinetic Battery Model (KiBaM)

Several modeling approaches can be found in the literature [11] - [13][25][30][31]. Some of them are devoted to the modeling of batteries and their lifetime estimation. The most commonly used model, called "performance model", is based on the battery state of charge (SoC) evaluation [14] [15]. The "voltage model" serves to estimate all the time the voltage of the battery. In general cases, it takes the losses into account. The "model of lifetime" can be obtained from aging experimental tests based on different scenarios [18] [19]. Some authors propose a combination of the previous model to improve the accuracy of the model in simulation and calculation [11] [20]-[23].

In this paper, the kinetic battery model (KiBaM) that was initially proposed by Manwell and McGowan (1993) [24] [11] [16] is studied due to its simplicity and good performances. But, much work remains to be done to improve the methodology for estimating of the weight of each degradation mechanism on the lifetime and for calculation of the model parameters. The KIBAM is defined by two parts named capacity and voltage models.

A. Capacity Model (CapMod)

The battery capacity can be modeled as a two tanks system with a cumulated capacity q, with different volumes, with unit depth and different widths. The tank 1 contains the capacity q_1 that is immediately available to supply energy while the tank 2 contains the capacity q_2 that is "chemically bound", according to (1). The conductance 'k' between the two tanks is defined as a first-order rate of a chemical reaction/diffusion process by which the bound charge becomes available. This rate is assumed proportional to the difference in "head" of the two tanks. The width of tank 1 is c, and that of tank 2 is (1-c). The initial capacities $q_{1,0}$ and $q_{2,0}$ are the amount of available and bound charge, respectively, with $q_0=q_{1,0}+q_{2,0}$. The nominal capacity q_{nom} corresponds to the absolute value of the maximum capacity of the battery at the limit of zero-current discharge (or charge), by assuming a constant current over the time step Δt.

$$\begin{cases} q_1 = q_{1,0} \cdot e^{-k\cdot\Delta t} + \dfrac{(q_0 \cdot k \cdot c - I)\cdot\left(1-e^{-k\cdot\Delta t}\right)}{k} - \dfrac{I\cdot c\cdot\left(k\cdot\Delta t - 1 + e^{-k\cdot\Delta t}\right)}{k} \\ q_2 = q_{2,0}\cdot e^{-k\cdot\Delta t} + q_0\cdot(1-c)\cdot\left(1-e^{-k\cdot\Delta t}\right) - \dfrac{I\cdot(1-c)\cdot\left(k\cdot\Delta t - 1 + e^{-k\cdot\Delta t}\right)}{k} \end{cases} \quad (1)$$

$$and \begin{cases} SoC = \dfrac{q}{q_{nom}} \\ DoD = 1 - \dfrac{q}{q_{nom}} \end{cases}$$

The state of charge (SoC) is defined as 0 ≤ SoC ≤ 1. The battery is fully discharged ("empty") when SoC = 0 and fully charged ("full") when SoC = 1.

B. Voltage Model (VoltMod)

The Voltage Model (VoltMod) is defined as a SoC dependant electromotive force E (emf) in series with a constant internal resistance R_0. The battery voltage decreases slowly and quasi-linearly in the first part of the discharge curve and decrease quickly after the knee, when the battery is nearly empty.

In (2), $q_{max}(I)$ is defined as the maximum discharge capacity at a given constant discharge current I, and q_{max} is the maximum possible capacity at I=0, provided by the manufacturer or estimated from experimental tests. E_0 is the full charged internal battery voltage, after the initial transient.

$$\begin{cases} V_{bat} = E - I_{bat}\cdot R_0 \\ E = E_0 + A\cdot X + \dfrac{C\cdot X}{D-X} \end{cases} \quad (2)$$

with

$$X = \begin{cases} q * q_{\max}/q_{\max}(I) & \text{charge} \\ q_{out} * q_{\max}/q_{\max}(I) & \text{discharge} \end{cases}$$

C. Method of the KiBaM Characterization

The parameters (E_0, A, C, D, c, k, q_{max}) of KiBaM model may be found by estimated from the Levenberg-Marquardt algorithm, applied to at least 3 sets of tests results of discharge process with constant current, according to Fig.2. The voltage drop ΔV_0 serves to calculate the internal resistance according to (3). The current expression of (3) serves to estimate the constants of the capacity model (c, k, Q_{max}). Tests are performed with constant current over the maximum discharge time, until the voltage curve begins to drop off sharply [28]. Then the maximum capacity is estimated.

$$\begin{cases} R_0 = \dfrac{\Delta V_0}{I} \\ I = \dfrac{k\cdot c\cdot q_{\max}}{1-e^{-k\cdot t} + c\cdot\left(k\cdot t - 1 + e^{-k\cdot t}\right)} = \dfrac{k\cdot c\cdot q_{\max}}{\gamma(t)} \end{cases} \quad (3)$$

III. Levenberg-Marquardt optimization method

Levenberg-Marquardt (L-M) optimization method is suitable to solve multivariable nonlinear systems. It serves to find the optimal solution that minimizes the objective function. The minimum is reached when the gradient of the objective function $f(x_k)$ is equal to zero, with the vector $x \in R^n$ of unknowns and x_i the value of x at the k-th iteration.
Let define the error vector, to minimize, as (4).

$$\varepsilon_k = f(x_k) \quad (4)$$

At each step, the vector of variables x is updated according to the variation Δx_k (5) and the Jacobian matrix J_k of the objective function, by considering the n x n unit matrix I.

$$\begin{cases} x_{k+1} = x_k + \Delta x_k \\ \Delta x_k = -[J_k^T * J_k + \beta I]^{-1} J_k^T \varepsilon_k \end{cases} \quad (5)$$

The number of the iterations necessary to reach the convergence depends on the value of the damping coefficient β [26]. A small positive of β initial value can be defined.
The L-M serves to estimate the optimal values of the battery model parameters (c, k, q_{max}, E_0, A, C, D) from experimental tests results.
The partial derivatives are calculate as (6) and (7) from the current expression (3).

$$\begin{cases} \dfrac{\partial I}{\partial c} = \dfrac{kq_{max}}{\gamma(t)} - \dfrac{kcq_{max}(kt - e^{-kt})}{\gamma^2(t)} \\ \dfrac{\partial I}{\partial k} = \dfrac{cq_{max}}{\gamma(t)}\alpha(t) \\ \dfrac{\partial I}{\partial q_{max}} = \dfrac{kc}{\gamma(t)} \end{cases} \quad (6)$$

With, $\alpha(t) = \dfrac{kcq_{max}te^{-kt}}{\gamma^2(t)} + ct\left(1 - e^{-kt}\right)$

$$\begin{cases} \dfrac{\partial E}{\partial E_0} = 1 \\ \dfrac{\partial E}{\partial A} = X \\ \dfrac{\partial E}{\partial C} = \dfrac{X}{D-X} \\ \dfrac{\partial E}{\partial D} = \dfrac{-CX}{(D-X)^2} \end{cases} \quad (7)$$

The iterative procedure of the parameters estimation is applied to the experimental tests results performed with constant current of discharge. At least three tests are necessary with different level of current. In Fig.2, it can be observed the voltage variation in discharge process at constant current.
The capacity removed q_{out} when voltage decrease from point A to B is estimated for each test current. Then, results of tests are used in the L-M optimization method for model parameters estimation.

IV. EXPERIMENTAL RESULTS

a. LEAC-ACID BATTERY MODELING

A PFX2021 module of Kikusui (Fig.3) is used for experimental tests of cycling and ageing of the battery. Ambient temperature can be controlled by a thermoelectric temperature chamber. Communication between the cycling test unit (CTU) and the climatic chamber is ensured by the RS485/RS232 converter. A control unit module is interfaced between the CTU and the Computer (PC). Dedicated software is used for system configuration and data storage on the computer. In the first experimental tests, two Depths of Discharge (DoD) are applied to a Valve Regulated lead-acid battery Yucel Y14-12 (14Ah, 12V) cycling. Discharge curves of the battery from 14v to 11v versus the charge removed are presented in Fig.4 for different currents values. Compared to a high level DoD of Fig.5, it appears a fast discharge slope after the discharge knee.

From Fig.6, it appears that the voltage drops, at the starting (ΔV_0) and at the end (ΔV) of the discharge process. The value of drop varies according to the current level.

$$\begin{cases} Diff_{\_14v1v} = \dfrac{\Delta V_{\_14v1v} - \Delta V_{0\_14v1v}}{\Delta V_{0\_14v11v}} \\ Diff_{\_14v11v} = \dfrac{\Delta V_{\_14v11v} - \Delta V_{0\_14v11v}}{\Delta V_{0\_14v11v}} \\ Diff_{\_V0} = \dfrac{\Delta V_{0\_14v1v} - \Delta V_{0\_14v11v}}{\Delta V_{0\_14v11v}} \\ Diff_{\_V} = \dfrac{\Delta V_{\_14v1v} - \Delta V_{\_14v11v}}{\Delta V_{0\_14v11v}} \end{cases} \quad (8)$$

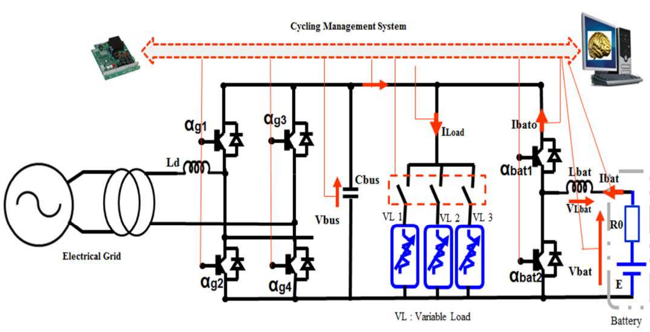

Fig.1. Electrical circuit of the battery cycling test bench.

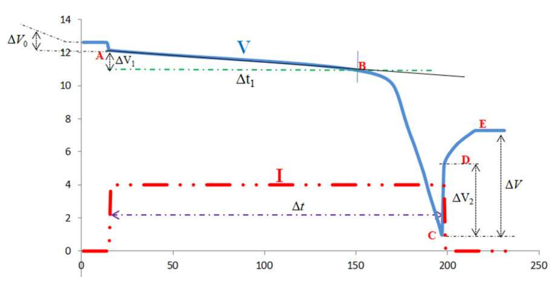

Fig. 2. Variables of the model parameters estimation, accroding to the time to voltage curve.

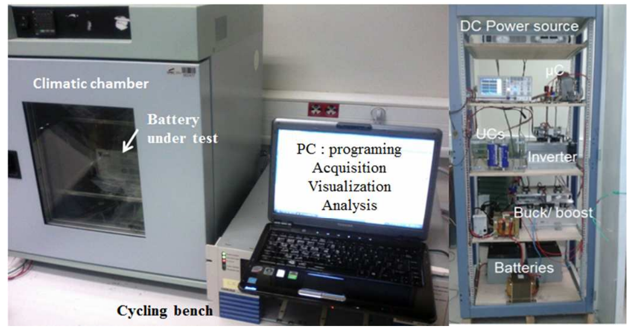

Fig. 3. Experimental tests bench of the battery cycling and ageing.

The voltage drop ΔV_{0_14v11v} is defined to serve a reference for comparison in the two cases of DoD, according to (8). Errors of estimation are presented in Fig.7 which shows that the voltage drop varies according to the current value.

i. APPROACHES OF INTERNAL RESISTANCE ESTIMATION

The internal resistance can be estimated from different ways according to (9) and Fig.8. For all cases, the value of the resistance is dependent to the current level.

$$\begin{cases} R_0 = \dfrac{\Delta V_0}{I} \\ R = \dfrac{\Delta V}{I} \\ R_2 = \dfrac{\Delta V_2}{I} \end{cases} \quad (9)$$

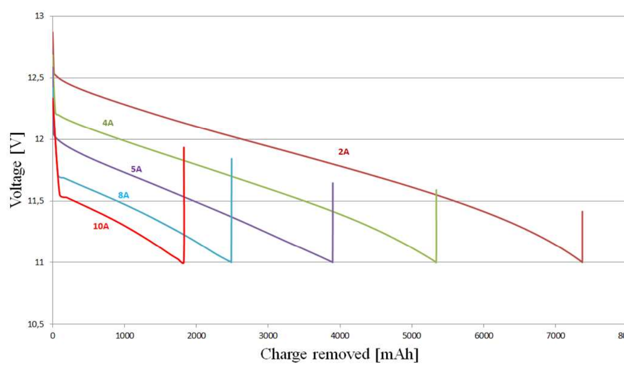

Fig.4 Removed charges to Voltage variation curve.

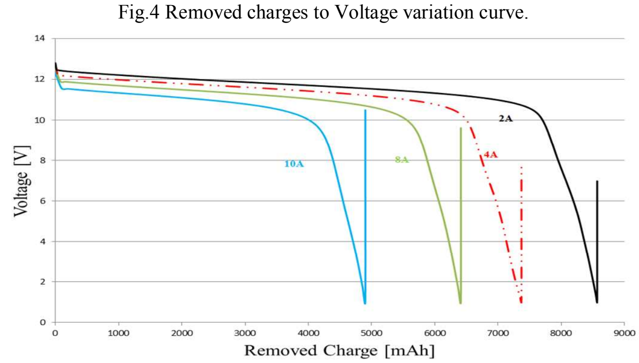

Fig.5 High DOD (14V-1V) effect on the voltage profile in discharge mode

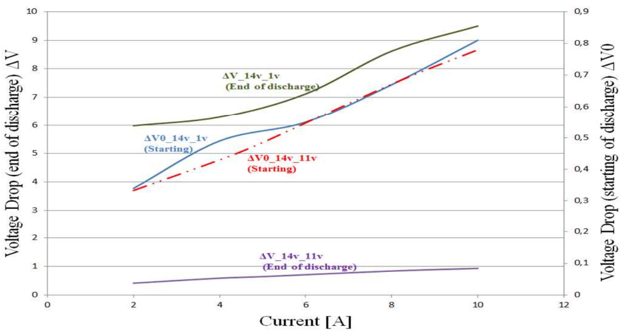

Fig.6 Voltage drop variation for each current level.

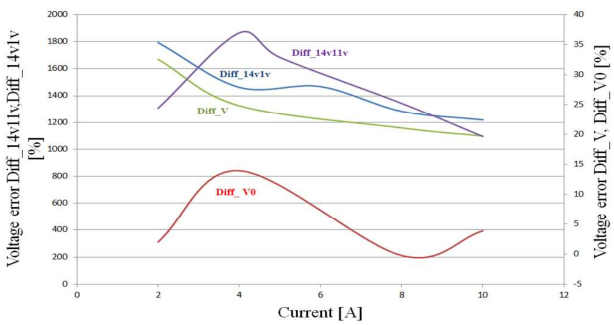

Fig. 7 : Errors between voltage drops in the two cases of DoD.

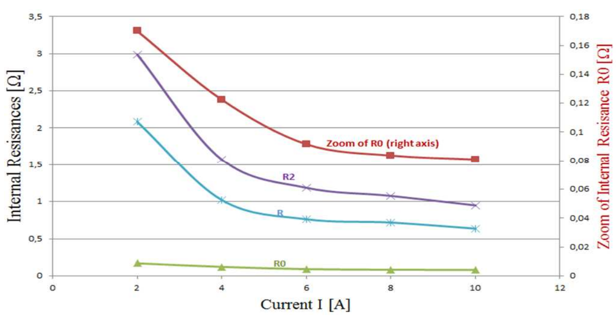

Fig. 8 : Variation of the internal resistance.

Results presented in Fig.9 are obtained from experimental test with 10A current, for voltage varying from 14V to 11V at three different, but narrow, values of temperature (26°, 27°, and 28° respectively for test 1 to 3).

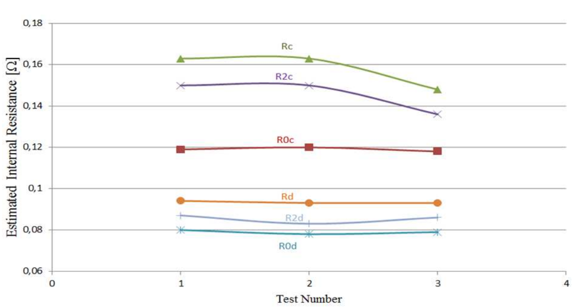

Fig. 9 : Effect of temperature on internal resistance for same current of 10A. Index "c" is for charge process and "d" for discharge case.

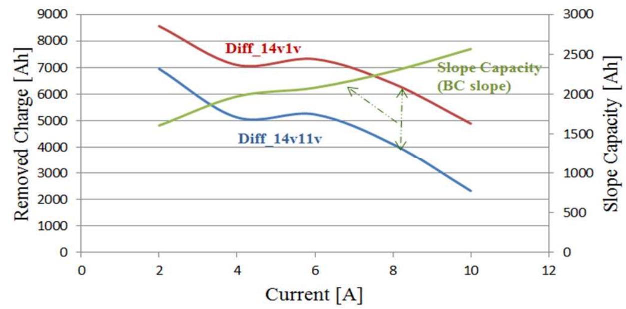

Fig. 10 : Charge removed vs. Current level and the slope capacity.

In Fig.10, different values of current are used to discharge the battery from 14v to 1V and from 14v to 11V. The difference between the two curves corresponds to the charges extracted from the slope phase occurring from 11V to 1V (section BC in Fig.2). This last is also presented in Fig. 11 with the corresponding ratio, related to the total charge removed for each current.

The variations of the floating voltage according to the current level are estimated in discharge case from 14v to 1v and linearized, as shown in Fig.12.

ii. Estimated parameters of the model

Results of the experimental tests are used to estimate the KIBAM model parameters presented in Table I and II. The output of the model is compared to the experimental discharge voltage in Fig.13, which shows a good approximation of curves and illustrates the efficiency of the parameters estimation method.

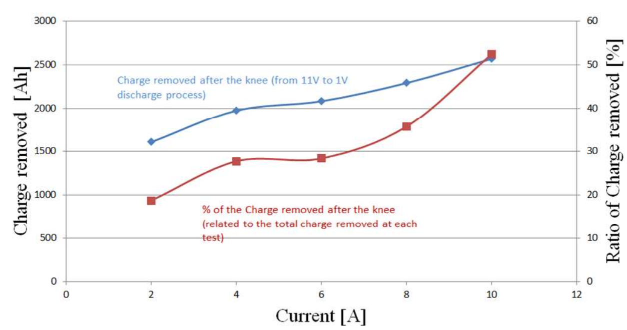

Fig. 11 : Variations of the charge recovered from the voltage slope

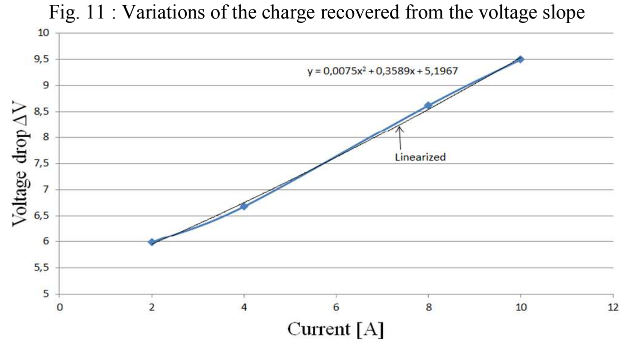

Fig. 12 : Variations of the floating voltage vs. the current at the end of discharge

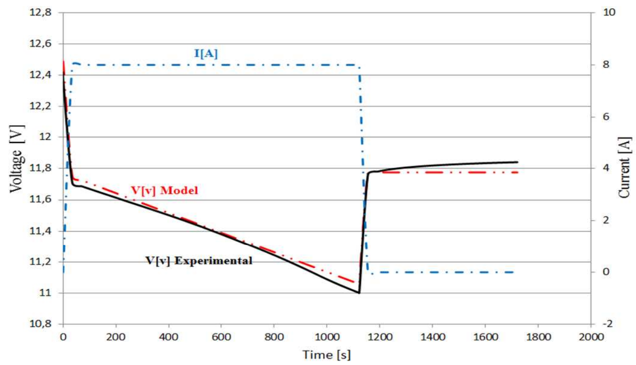

Fig. 13 : Performance of the model compared to the experimental voltage.The two signals are very closed due to the good estimation of the simulation model parameters.

TABLE I. PARAMETERS OF THE VOLTAGE MODEL

E0	*A*	*C*	*D*	*R0 (Ω)*	*ΔV0 (V)*
12,489	-5,09E-05	4,39E-06	15000	0,089875	0,719

TABLE II. PARAMETERS OF THE CAPACITY MODEL

c	**k**	**Qmax (mAh)**
0.06915	0.0193	14000

b. LITHIUM ION BATTERY MODELING

Tests are performed with a 5200 mAh Lithium ion battery. Effect of the discharge current levels can be observed in Fig. 5. The voltage increase with the current value and the knee points are not the same. For each of the batteries, discharge tests at different discharge currents are performed per period of 25 cycles in aim to determine the aging characteristics at regular intervals. The slope of the lithium-ion in Fig.14 is less linear than the slope of the lead-acid batteries presented in Fig. This can induce more dispersion of the measured values than in case of the lead acid batteries. An adaptation of the initial model is realized by adding a manual adjustment phase based on the observation and comparison, this makes it possible to improve the precision of the model parameters. By applying the method presented above, combined with a manual adjustment, the parameters of the lithium-ion battery estimated are shown in Table III.

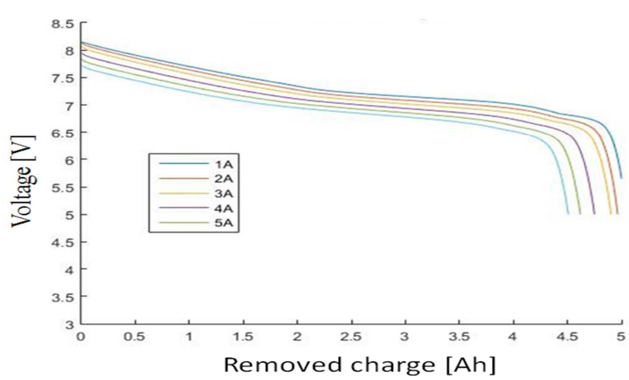

Fig. 14 : Voltage variation of lithium-ion battery according to discharge currents and charge removed.

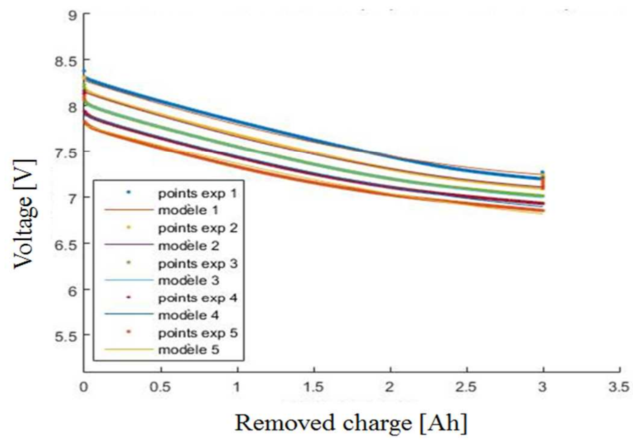

Fig.15: Comparison between experimental tests and results of the established model of Li-ion for different currents

By applying the method presented above, combined with a manual adjustment, the parameters of the lithium-ion battery estimated are shown in Table III. Tests are doing with constant current for 10, 25 and 48 aging cycles over a discharge depth of 80%. The slight variations of some parameters are compensated by those of the other parameters. Thus, the limited number of cycles does not allow observing degradation of the behavior. So, the parameters of the model can be defined for one or more number of cycles (less than ten cycles) without big changes between them. In Fig.15, curves obtained from the model are compared to the experimental results, for each discharge current considered and varying from 0.5A (model 1) to 2.5A (model 5) with incremental increment of 0.5A. Good precision is observed between the experimental curves and those of the corresponding model.

TABLE III. PARAMETERS OF THE VOLTAGE AND CAPACITY MODELS OF THE LI-ION BATTERY

Parameters	**cycle 10**	**cycle 25**	**cycle 48**
c	0.83	0.824	0.886
k	39.4	35	42
A	-1.434	-2.2	-1.64
E_0	8.2	8.07	8.14
C	23.03	75.1	30.9
q_{max}	3.01	3.53	3.49
D	23.7	42.5	26.2
R_0	0.114	0.092	0.093

V. CONCLUSIONS

In this paper, behaviours of the lead-acid and lithium-ion batteries are studied. The provided experimental results are used in the design of a simulation model and of a Battery Management System (BMS) which can take into account impacts of the micro-cycles on the batteries lifetime. This can help to define the decision rules and the batteries lifetime estimation tools. Tests are performed with a constant current.

From experimental results, for each value of test current, following behaviors are observed:

From all the experimental tests carried out with a constant current, it will be able to make the following observations:
- a voltage variation as a linear function of the removed charge;
- a decrease of the charging voltage and a variation of the discharge modes according to the actual SOC. Their values at the beginning of each mode are very small compared to the end of the modes (when the current becomes zero);
- the values of the estimated internal resistance vary according to the temperature level, to the operating mode (charge or discharge) and to the voltage drop considered. Small values are found when using voltage drop at the mode starting (charge or discharge) with linear variations as a function of temperature. The weakest values of resistance are observed in case of discharge mode;
- the floating voltage depends on the value of the discharge current;
- a large quantity of charges (20% to 50%) can be extracted in the part of the time-based slope of the voltage. The operation in the quasi-linear part makes it possible to reduce the life of the battery, it is the most advisable to optimize the batteries lifetime. Nevertheless, a complete study is necessary to verify the impacts induced by operation beyond the curvature of the slope.

The estimated parameters of the model can provide a very good approximation of the experimental behavior of the battery. The models of the established batteries are used for simulations under Matlab / simulink for behavioral analysis but also for design calculations. Thus, they can help to the choice between technologies (lead-acid and Li-ion) by taking into account their dynamics in conventional sizing calculations based on the minimization of energy costs.

REFERENCES

[1] J. Randolph and G. M. Masters, “Energy for sustainability, technology, planning, policy,” Island Press, 2008.

[2] J. Kabouris and F. D. Kanellos, “Impacts of Large-Scale Wind Penetration on Designing and Operation of Electric Power Systems,” *IEEE Trans. on Sustainable Energy*, vol. 1, no. 2, pp. 107-114, July 2010.

[3] W. Li, G. Joos, and J. Bélanger, “Real-Time Simulation of a Wind Turbine Generator Coupled With a Battery Supercapacitor Energy Storage System,” IEEE Transactions On Industrial Electronics, vol. 57, no. 4, pp. 1137 - 1145, April 2010.

[4] M. A. Tankari, M. B. Camara; B. Dakyo; G. Lefebvre, "Use of Ultracapacitors and Batteries for Efficient Energy Management in Wind-Diesel Hybrid System ", *IEEE Transactions on Sustainable Energy*, *ITSEAJ ISSN 1949-3029,* Vol.4, N°2 pp.1 - 11, April 2013.

[5] M. A. Tankari, M.B.Camara, B. Dakyo, C. Nichita, “Wind Power Integration in Hybrid Power System with Active Energy Management”, *International Journal for Computation and Mathematics in Electrical and Electronic Engineering (COMPEL)*, Vol. 30, No. 1, 2011, pp. 245-263.

[6] Z. Guoju, T. Xisheng, and Q. zhiping, “Research on Battery Supercapacitor Hybrid Storage and its application in MicroGrid,” *in Proc. IEEE Asia-Pacific Power and Energy Engineering Conf. (APPEEC),* pp. 1-4, 2010.

[7] K. John and F. D. Kanellos, “Impacts of Large-Scale Wind Penetration on Designing and Operation of Electric Power Systems,” *IEEE Trans. Sustainable Energy,* vol. 1, no. 2, pp. 107- 114, July 2010.

[8] M. Bragard, N. Soltau, S. Thomas, and R. W. De Doncker, “The Balance of Renewable Sources and User Demands in Grids: Power Electronics for Modular Battery Energy Storage Systems,” *IEEE Trans Power Electronics,* Vol. 25, No. 12, December 2010, pp. 3049—3056.

[9] C. Abbey, W. Li, and Géza Joós, “An Online Control Algorithm for Application of a Hybrid ESS to a Wind–Diesel System,” *IEEE Trans Industrial Electronics*, vol. 57, no. 12, pp. 3896, Dec. 2010.

[10] S. Teleke, M. E. Baran, S. Bhattacharya, and A. Q. Huang, “Optimal Control of Battery Energy Storage for Wind Farm Dispatching,” *IEEE Trans. Energy Conversion,* vol. 25, no. 3, pp. 787- 794, September 2010.

[11] H. Bindner, T. Cronin, P.Lundsager, J. F. Manwell, U. Abdulwahid, I. Baring-Gould; “Benchmarking – Lifetime Modelling;” *ENK6-CT-2001-80576*; April 2005.

[12] A. Jossen, Fundamentals of battery dynamics, *Journal of Power Sources*, no.154, pp. 530–538, 2006.

[13] V. Svoboda, et al., Operating conditions of batteries in off-grid renewable energy systems, *Journal of Solar Energy*, no. 81 pp. 1409–1425, 2007

[14] T. Christen, Martin W. Carlen; “Theory of Ragone plots”, *Journal of Power Sources*, no. 91, pp. 210–216 ; March 2000

[15] N. Jantharamin, L. Zhang, “A New Dynamic Model for Lead-Acid Batteries”, *4th IET Conference Power Electronics, Machines and Drives PEMD 2008*, pp. 86 – 90, York 2008.

[16] A. D. Hansen, P. Sorensen, L. H. Hansen, and H. Bindner; “Models for a stand-alone PV system”, *RISO-R-1219 (EN)/SEC-R-12; RISO National Laboratory, Roskilde*, Dec. 2000.

[17] M. Thele, S. Buller, D.U. Sauer, R.W. De Doncker, and E. Karden, “Hybrid modeling of lead–acid batteries in frequency and time domain”, *Journal of Power Sources*, no. 144, pp. 461–466, 2005.

[18] Y. H. Sun, H. L. Jou, J. C. Wu, “Intelligent Aging Estimation Method for Lead-Acid Battery”, *IEEE 8th International Conference on Intelligent Systems Design and Applications*, pp. 251-256, 2008.

[19] S. Drouilhet, B.L. Johnson, “A Battery Life Prediction Method for Hybrid Power Applications”, In Proc. *35th AIAA Aerospace Sciences Meeting and Exhibit Reno*, Nevada; Jan. 1997.

[20] J. Schiffer, D. U. Sauer, H. Bindner, T. Cronin, P. Lundsager, and R. Kaiser, “Model prediction for ranking lead-acid batteries according to expected lifetime in renewable energy systems and autonomous power-supply systems”; *Journal of Power Sources*, no168 , pp. 66–78, 2007

[21] M. D. M. Ross, "A Simple but Comprehensive Lead-Acid Battery Model for Hybrid System Simulation", *Proceedings of PV Horizon: Workshop on Photovoltaic Hybrid Systems, Montréal, Quebec*, Sept. 2001.

[22] N. Picciano, “Battery Aging and Characterization of Nickel Metal Hydride and Lead Acid Batteries” ,*Thesis, Ohio State University*, 2007

[23] A. Szumanowski and Yuhua Chang, Battery Management System Based on Battery Nonlinear Dynamics Modeling, *IEEE Transactions On Vehicular Technology*, vol. 57, no. 3, pp. 1425-1432, May 2008

[24] J. F. Manwell, A. Rogers, G. Hayman, C. T. Avelar, J. G. McGowan, U. Abdulwahid, and K. Wu; “Hybrid2- A Hybrid System Simulation Model - Theory Manual”, *Renewable Energy Research Laboratory, University Of Massachusetts*, June 2006.

[25] M. Ceraolo, “New Dynamical Models of Lead–Acid Batteries”, *IEEE Transactions Power Systems*, vol. 15, no. 4, pp.1184-1190, November 2000.

[26] Analogy and Convergence of Levenberg's and Lyapunov-based Methods for Power Flow Analysis, IEEE Transactions on Power Systems, Vol. 31, No. 2, pp. 1663-1664, March 2016.

[27] M.R. Jongerden, et al., "Maximizing System Lifetime by Battery Scheduling", In Proceedings of the 39th Annual IEEE/IFIP International Conference on Dependable Systems and Networks, DSN 2009, IEEE Computer Society Press, pp. 63-72, no.10, ISBN 978-1-4244-4421-2.

[28] Z. Nouhou Bako, M. Abdou Tankari, G. Lefebvre, A. Seidou Maiga, "Lead-acid battery behavior study and modelling based on the Kinetic Battery Model approach", 5th IEEE International Conference on Renewable Energy Research and Applications (ICRERA'16), pp. 673-677, Birmingham - United Kingdom 2016.
[29] S. A. Saleh, R. Meng, and R. McSheffery, "Evaluating the Performance of Digital Modular Protection for Grid-Connected Permanent Magnet Generator-Based Wind energy conversion Systems with Battery Storage Systems", IEEE Transactions on Industry Applications, Vol. 53, Issue 5, Sept.-Oct. 2017.
[30] J. V. Barreras; *et al*., "An advanced HIL Simulation Battery Model for Battery Management System Testing", IEEE Transactions on Industry Applications, Vol.52, Issue 6, pp.5086-5099, 2016.
[31] J. V. Barreras, *et al.,* “Evaluation of a novel BEV concept based on fixed and swappable Li-ion battery packs”, IEEE Transactions on Industry Applications, Vol.52, Issue 6, pp. 5073 – 5085, 2016.
[32] D. I. Stroe, *et al.,* “Degradation Behavior of Lithium-Ion Batteries based on Lifetime Models and Field Measured Frequency Regulation Mission Profile”, IEEE Transactions on Industry Applications, Vol.52, Issue 6, pp.5009 – 5018, 2016.